Importance of O vacancies in the behavior of oxide surfaces: Adsorption of sulfur on $TiO_2(110)$

José A. Rodriguez,* Jan Hrbek, Zhipeng Chang, Joseph Dvorak, and Tomas Jirsak
Department of Chemistry, Brookhaven National Laboratory, Upton, New York 11973

Amitesh Maiti
Accelrys, 9685 Scranton Road, San Diego, California 92121

(Received 14 November 2001; revised manuscript received 5 February 2002; published 28 May 2002)

Synchrotron-based high-resolution photoemission, thermal desorption mass spectroscopy, and first-principles density functional calculations were used to study the adsorption and reaction of sulfur with $TiO_2(110)$. At 100–300 K, S atoms bond much more strongly to O vacancy sites than to atoms in the Ti rows of a perfect oxide surface. The electronic states associated with Ti^{3+} sites favor bonding to S, but there is not a substantial oxide→adsorbate charge transfer. In general, the bond between S and the Ti cations is best described as covalent, with a small degree of ionic character. For dosing of S at high temperatures (>500 K) a layer of TiS_x is formed on $TiO_2(110)$. The O signal disappears in photoemission and Auger spectroscopy, and the Ti $2p$ core levels show a complete $TiO_2 \rightarrow TiS_x$ transformation. The O↔S exchange does not involve the production of SO or SO_2 species. Instead, the formation of TiS_x involves the migration of O vacancies from the bulk to the surface. The $S/TiO_2(110)$ system illustrates how important can be surface and subsurface defects in the behavior of an oxide surface. The exchange of O vacancies between the bulk and surface can lead to unexpected chemical transformations.

DOI: 10.1103/PhysRevB.65.235414 PACS number(s): 68.43.−h; 68.47.Gh; 82.33.Pt; 82.45.Jn

I. INTRODUCTION

The adsorption of molecules on oxide surfaces is a key process in the fabrication of electronic devices, catalysis, photoelectrolysis, corrosion, sensor development, etc.[1,2] The metal elements are able to form a large diversity of oxide compounds.[1,2] These oxides adopt a vast number of structural geometries and at an electronic level they can exhibit metallic character or behave as semiconductors or insulators.[1,2] Recent theoretical studies have demonstrated the important role that oxygen vacancies play in the behavior of highly ionic oxides like MgO or Al_2O_3.[3–8] In their pure stoichiometric states, these oxides exhibit large band gaps, with bands that are either too stable (valence states) or unstable (conduction states) for effective bonding interactions with most adsorbates.[9] On highly ionic oxides, the binding of an adsorbate is frequently due to pure electrostatic interactions with the oxide substrate.[1,9–11] The presence of O vacancies induces electronic states within the oxide band gap[3,4] that make possible bonding interactions with the orbitals of adsorbates.[3,9] In the case of MgO(100), the excess electronic charge is highly localized on the O vacancy sites,[3,4,12] and a large fraction of it can be transferred to adsorbates.[3,5,8] In a much less ionic oxide like TiO_2,[1,13,14] the degree of charge localization on the O vacancy sites is less pronounced and part of the excess electronic charge is distributed on the neighboring cations.[14–16] It is not obvious what behavior to expect for adsorption on this type of system or how important can be the adsorbate↔vacancy interactions for the chemical properties of the oxide surface. To address these issues, in this article we examine the bonding of sulfur to stoichiometric and partially reduced $TiO_2(110)$ surfaces.

In general, a fundamental understanding of the interaction of sulfur with oxide surfaces is important for two practical reasons.[17–21] First, in several operations in the semiconductor industry sulfur is deposited on oxide surfaces to passivate or protect electronic devices.[1,17] Second, oxides are frequently used as sorbents or catalysts to remove sulfur-containing molecules from the oil and to prevent the evolution into the atmosphere of the SO_2 formed as a by-product during the combustion of fuels.[1,18–21] In practical terms, it is necessary to establish what types of oxides have a high reactivity toward sulfur.[17,18,20] In spite of this, very few studies have appeared examining in detail the bonding of sulfur to well-defined oxide surfaces.[1,22–27] TiO_2 is employed on a large industrial scale for the removal of H_2S and SO_2 in the Claus process.[21] Previous works have investigated the adsorption of SO_2,[28–31] H_2S,[29] and elemental sulfur,[24–27] on $TiO_2(110)$.

Results of scanning tunneling microscopy (STM) indicate that at room temperature S adsorbs on the titanium rows of the $TiO_2(110)$ surface with a high mobility along the [001] direction.[24] The formation of TiS_x aggregates was observed on the oxide surface after dosing sulfur at elevated temperatures (> 500 K).[24,26] The exact details of the mechanism for the formation of TiS_x are unclear. It was proposed that the migration of O vacancies or Ti^{3+} interstitials from the bulk to the surface of the oxide could play a role in the generation of TiS_x,[26] but a surface reaction of the $S_2 + TiO_2 \rightarrow TiS + SO_2$ type could not be ruled out with the existing STM or x-ray photoelectron spectroscopy data. In this article we use a combination of synchrotron-based high-resolution photoemission, thermal desorption mass spectroscopy (TDS), and first-principles density functional calculations to study the

properties of the $S/TiO_2(110)$ system. Our results show important changes in the nature of the S-TiO_2 bond depending on the sulfur coverage, adsorption site, and temperature of the surface. The S $2p$ core levels are very sensitive to changes in the chemical environment around the S atoms. A complete $TiO_2 \rightarrow TiS_x$ transformation is observed within the escape depth probed by photoemission. The present results illustrate how O vacancies localized in the subsurface region of an oxide can drive chemical transformations that would be impossible in a stoichiometric material.

The article is organized as follows. Section II contains a description of the technical details of the work, including the experimental and theoretical methods used. Section III starts with a presentation of photoemission and TDS spectra for $S/TiO_2(110)$, followed by an analysis of first-principles calculations for this system. In Sec. IV, we discuss our data and general trends that show the importance of surface and subsurface vacancies for the behavior of $TiO_2(110)$ and other oxide surfaces.

II. EXPERIMENTAL AND THEORETICAL METHODS

A. Photoemission and TDS experiments

The experiments described in Sec. III A were carried out in two separate ultrahigh-vacuum (UHV) chambers. The photoemission spectra were acquired at the National Synchrotron Light Source (NSLS) using beamline U7A. The end station of this beamline consists of an UHV chamber (base pressure $<7\times10^{-10}$ Torr) fitted with a multichannel electron-energy analyzer for photoemission, optics for low-energy electron diffraction (LEED), and a quadrupole mass spectrometer.[32] The S $2p$ and Ti $2p$ photoemission data were acquired using photon energies of 260 and 625 eV, respectively. The binding energy scale in the spectra was calibrated by the position of the Fermi edge. The overall instrumental resolution in the photoemission experiments was 0.3–0.4 eV. A second UHV chamber (base pressure $<3\times10^{-10}$ Torr) was equipped with an Auger electron spectrometer (AES), LEED, and instrumentation for TDS. The same TiO_2 crystal mounted in a Ta frame and sandwiched between Ta plates was spot welded to Ta heating legs of a manipulator capable of cooling to 80 K and heating to 1185 K and used in both chambers.

The $TiO_2(110)$ crystal was cleaned following procedures described in the literature[23,27] that consisted of initial sample heating to 1000 K for 1 h, with subsequent cycles of sputtering (1 keV Ne^+ ions) at room temperature and 10 min anneal at 970–1000 K in UHV. This preparation leads to a dark blue crystal with no detectable impurities as judged by AES and photoemission. The sample exhibited a (1×1) LEED pattern, and previous studies using STM (Ref. 24) and photoemission[27,33] have shown that the resulting surface has O vacancies in the bridging oxygen rows with a density of $\sim$7%. This partially reduced $TiO_2(110)$ surface was exposed to S_2 at temperatures between 100 and 800 K. S_2 gas was generated *in situ* by decomposing Ag_2S in a solid-state electrochemical cell $Pt/Ag/AgI/Ag_2S/Pt$.[32]

B. First-principles density functional calculations

The geometries and bonding energies for sulfur on stoichiometric and partially reduced $TiO_2(110)$ were calculated using the CASTEP (Cambridge serial total energy package) code.[34,35] Previous work indicates that CASTEP can be quite useful for studying adsorption processes on $TiO_2(110)$,[33,36–39] and on other oxide surfaces.[5,40–42] In this code, the Kohn-Sham equations are solved within the framework of density functional theory by expanding the wave functions of valence electrons in a basis set of plane waves with kinetic energy smaller than a specified cutoff energy E_{cut}.[34,35] The presence of tightly bound core electrons is represented by nonlocal ultrasoft pseudopotentials of the Vanderbilt type.[43] The valence s and p states of O and S, and the semicore $(3s,3p)$ and valence $(3d,4s,4p)$ states of Ti are explicitly treated. Reciprocal-space integration over the Brillouin zone is approximated through a careful sampling at a finite number of k points using the Monkhorst-Pack scheme.[44] In all the calculations, the kinetic energy cutoff ($E_{cut}=400$ eV) and the density of the Monkhorst-Pack k-point mesh [a $8\times4\times1$ grid for the smallest (1×1) surface unit cell, reduced to $4\times4\times1$ or $4\times2\times1$ grids for larger cells] were chosen high enough to ensure convergence of the computed structures and energetics. The exchange-correlation contribution to the total electronic energy is treated in a generalized gradient corrected (GGA) extension of the local density approximation (LDA).[45] We have used the GGA functional in the form proposed by Perdew and Wang.[45,46] This functional should give reasonable predictions for the bonding energies of sulfur on $TiO_2(110)$.[3,9,38,39,42] For the bonding of small molecules to $TiO_2(110)$ the Perdew-Wang functional predicts adsorption energies that are within 0.25 eV of the experimental values.[33,38,39] In this work, our main interest is in the relative energy changes with sulfur adsorption site and sulfur coverage, not in absolute values.

The structural parameters of the $S/TiO_2(110)$ system in its different configurations were determined using the Broyden-Fletcher-Goldfarb-Shanno minimization technique, with the following thresholds for the converged structures: energy change per atom less than 5×10^{-6} eV, residual force less than 0.02 eV/Å, and displacement of atoms during the geometry optimization less than 0.001 Å. For each optimized structure, the partial charges on the atoms were estimated by projecting the occupied one-electron eigenstates onto a localized basis set with a subsequent Mulliken population analysis.[47] The Mulliken charges must not be interpreted in absolute quantitative terms because of the uncertainty in uniquely defining a charge-partitioning scheme.[47]

III. RESULTS

A. Adsorption of sulfur on $TiO_2(110)$: Photoemission and thermal desorption studies

Figure 1 shows S $2p$ photoemission spectra acquired after dosing S_2 to a $TiO_2(110)$ surface at 100 K. For the smallest dose a doublet is observed with the S $2p_{3/2}$ features at

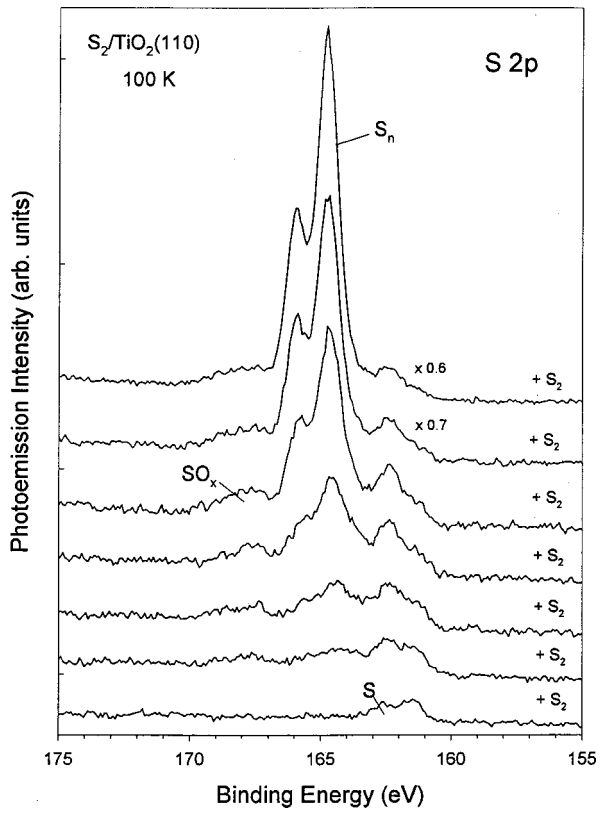

FIG. 1. S $2p$ photoemission spectra for the adsorption of S_2 on $TiO_2(110)$ at 100 K.

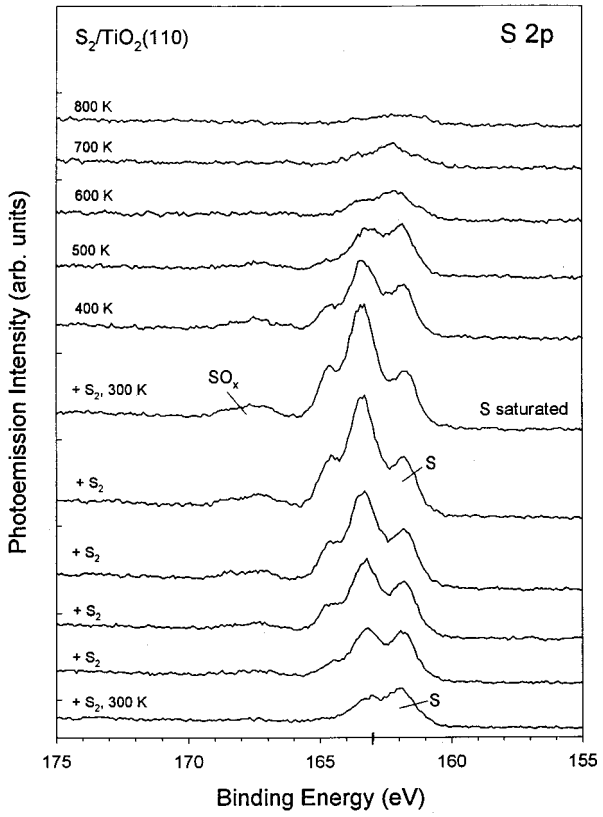

FIG. 2. S $2p$ photoemission spectra for the adsorption of S_2 on $TiO_2(110)$ at 300 K, with subsequent heating to the indicated temperatures (300–800 K).

~161.5 eV. This denotes the presence of S atoms adsorbed on O vacancies.[25] Thus, these sites are reactive enough to dissociate S_2 at 100 K. Additional dosing of sulfur leads to the appearance of features near 164 and 167.5 eV. The latter match the binding energy position for SO_3 species on oxides[48] and, since they saturate with a very small intensity, can be assigned to S atoms that react with O sites near defects of the surface. (A peak for a direct reaction of S with atoms in the O bridging rows should be much stronger.) The features between 166 and 164 eV agree with the position found for S_n species on metal and oxide surfaces.[39,49] Once the O vacancies are saturated with sulfur, the S_2 molecules start to adsorb on the Ti rows and instead of dissociating, they form S_n aggregates.

Figure 2 displays S $2p$ data for the adsorption of S_2 on $TiO_2(110)$ at 300 K, with subsequent annealing to higher temperatures. Initially, sulfur adsorbs on the O vacancy sites. Additional dosing leads to a sulfur saturation coverage of 0.6–0.7 monolayers (ML) on the oxide surface[24,25] and complex S $2p$ features. At this point, the S $2p$ spectrum is well fitted by a set of four doublets (see bottom of Fig. 3) with $2p_{3/2}$ components at 161.6(d_1), 162.8(d_2), 163.3(d_3), and 167 eV(d_4). To fit these data a Shirley background was subtracted from the raw spectrum, and a convolution of Lorentzian and Gaussian functions was used to fit each peak.[32,48,49] The d_1 doublet is assigned to S atoms on O vacancies.[25] The d_4 doublet likely corresponds to SO_3 groups.[48] The difference in binding energy between the d_2 and d_3 doublets is only ~0.3 eV, and following previous STM studies[24] we assign these features to S atoms bonded to the Ti rows of the surface. These atomic sulfur species clearly appear at binding energies different (1.0–1.5 eV) from those of the S_n aggregates seen at 100 K in Fig. 1. Upon heating from 350 to 550 K (Fig. 2), the S bonded to the Ti rows disappears from the surface and only the S bonded to O vacancy sites remains adsorbed.

Data for the desorption of sulfur from $S/TiO_2(110)$ surfaces are shown in Fig. 4. The left-side panel shows the effects of temperature on the S $2p$ intensity for surfaces prepared by adsorbing sulfur at 100 and 300 K. In both cases the largest drop in S $2p$ intensity is seen between 350 and 550 K. The right-side panel in Fig. 4 shows typical S_2 and S TDS spectra for $S/TiO_2(110)$ (sulfur adsorption at 300 K). Evolution of S_2 (mass 64, see below) into the gas phase is seen from 350 to 500 K, as a consequence of desorption of S atoms from the Ti rows ($2S_{ads} \rightarrow S_{2,gas}$). Evolution of atomic S into the gas phase occurs from 350 to almost 800 K in a broad and weak trace. Thus, S atoms bonded to O vacancy sites of $TiO_2(110)$ desorb as atomic species. No TDS spectra have been reported for the desorption of sulfur from other oxide surfaces, but in the case of sulfur adsorbed on metals evolution of S_2 and S has been observed in TDS.[50,51] S_2 and SO_2 have mass 64 as the main peak in mass spectroscopy. The cracking of SO_2 in the mass spectrometer is expected to produce a peak at mass 48 for the SO fragment. In the TDS spectra for $S/TiO_2(110)$, the signal for mass 48 was negligible, well within the noise level of our instrument. There-

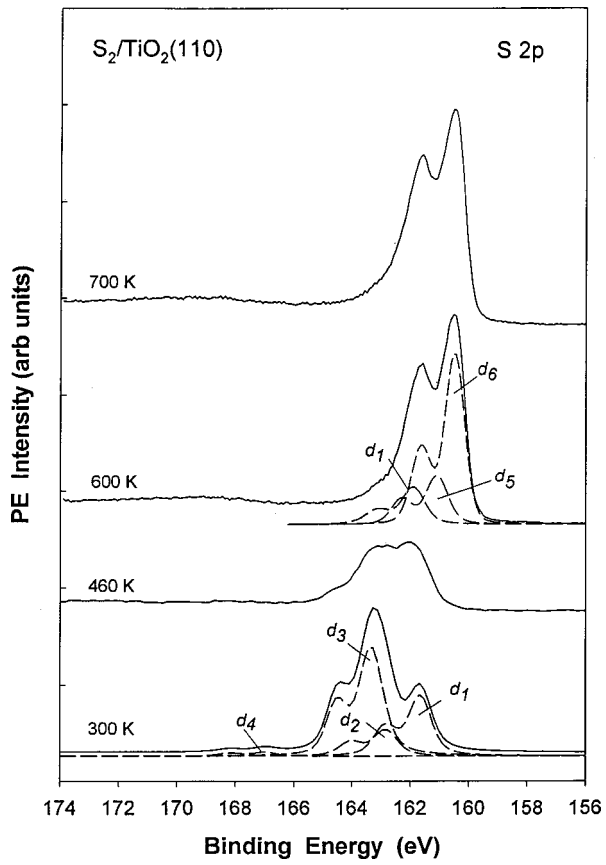

FIG. 3. S $2p$ photoemission spectra for saturation coverages of sulfur on $TiO_2(110)$ at 300, 460, 600, and 700 K. To fit the spectra a Shirley background was subtracted from the raw spectra, and a convolution of Lorentzian and Gaussian functions was used to represent each peak.

fore, we can conclude that the removal of surface O as SO_2 or SO gas is not an important channel when heating $S/TiO_2(110)$ surfaces.

An identical conclusion can be reached by analyzing the corresponding Ti $2p$ photoemission spectra (left panel in Fig. 5). After saturating the oxide with sulfur at 300 K, one sees an attenuation of the Ti $2p$ peaks without new features in the 456–457 eV region where Ti^{3+} species appear.[27,33] These extra features are also not seen when the sample temperature is raised from 300 to 500 K and species with mass 64 (S_2, no SO_2) evolve into the gas phase.

Hebenstreit *et al.* have observed the formation of TiS_x aggregates on $TiO_2(110)$ after dosing sulfur at elevated temperatures ($>$ 500 K).[24,26] Our experiments indicate that, in fact, all the oxygen atoms within the escape depth probed by photoemission can be replaced by S atoms. The Ti $2p$ photoemission data in the right-side panel of Fig. 5 for the dosing of sulfur at 700 K show trends clearly different from those seen for dosing at 300 K (left panel): new features appear, and the peaks for TiO_2 completely disappear when the surface is saturated with sulfur. Figure 6 shows AES spectra recorded after saturating $TiO_2(110)$ with sulfur at different temperatures. At room temperature, the sulfur is weakly bonded to the surface and the electrons from the AES gun induced partial desorption of the adsorbate. But, as the temperature of the sample is raised, S is bonded more strongly and the S *LMM* Auger signal increases. The intensity of the Ti *LMM* signal is not affected, but the O *KLL* signal disappears when sulfur is dosed at temperatures above 600 K. An identical phenomenon was observed in the O $1s$ photoemission spectra. All these results together indicate that there is a complete O↔S exchange at the surface and subsurface regions.

Figure 3 displays S $2p$ spectra for the saturation of $TiO_2(110)$ with sulfur at 300, 460, 600, and 700 K. As the sample temperature varies, there is a substantial change in the amount of sulfur adsorbed and in the position of the S $2p$ features. After background subtraction, the spectra at 600 and 700 K are well fitted by a set of three doublets with $2p_{3/2}$ components at 161.9 (d_1), 161.1 (d_5), and 160.5 eV (d_6). The d_1 features appear in a position that is close to that found at 300 K for S atoms bonded to vacancies on the bridging O rows. At elevated temperatures, the d_6 doublet is clearly dominant and exhibits a binding energy much lower than the binding energies seen for the species obtained after dosing sulfur at 300 K (d_1-d_4). The d_6 features are the ''fingerprint'' for the formation of TiS_x on the surface. They could originate in S atoms that replace the in-plane oxygens of the $TiO_2(110)$ surface. STM images[24,26] and first-principles calculations (next section) indicate that this should be the last stage in the sulfidation process. The results in Fig. 3 show that the S $2p$ core levels are very sensitive to changes in the chemical environment around the S atoms. This is consistent with the results of density functional (DF) calculations (next section) which point to significant changes in the nature of the S-TiO_2 bond depending on the adsorption site and sulfur coverage.

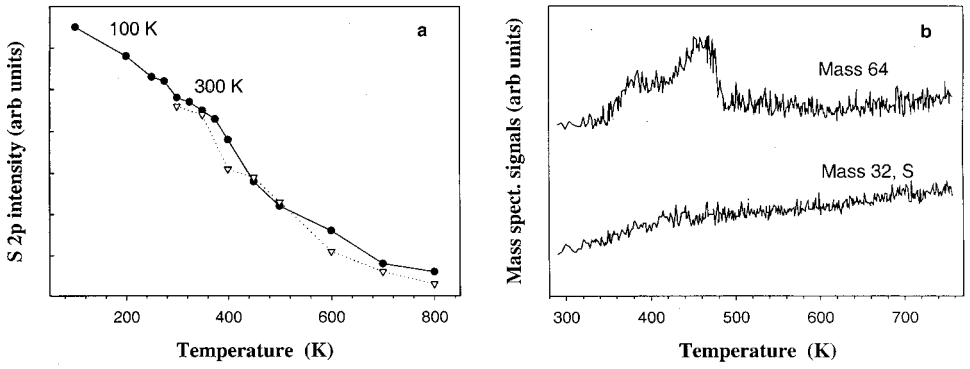

FIG. 4. Left side: Variation of the S $2p$ intensity with temperature after dosing S_2 to $TiO_2(110)$ at 100 and 300 K. Right side: Thermal desorption spectra for a $S/TiO_2(110)$ surface prepared at 300 K. Heating rate = 2 K/s.

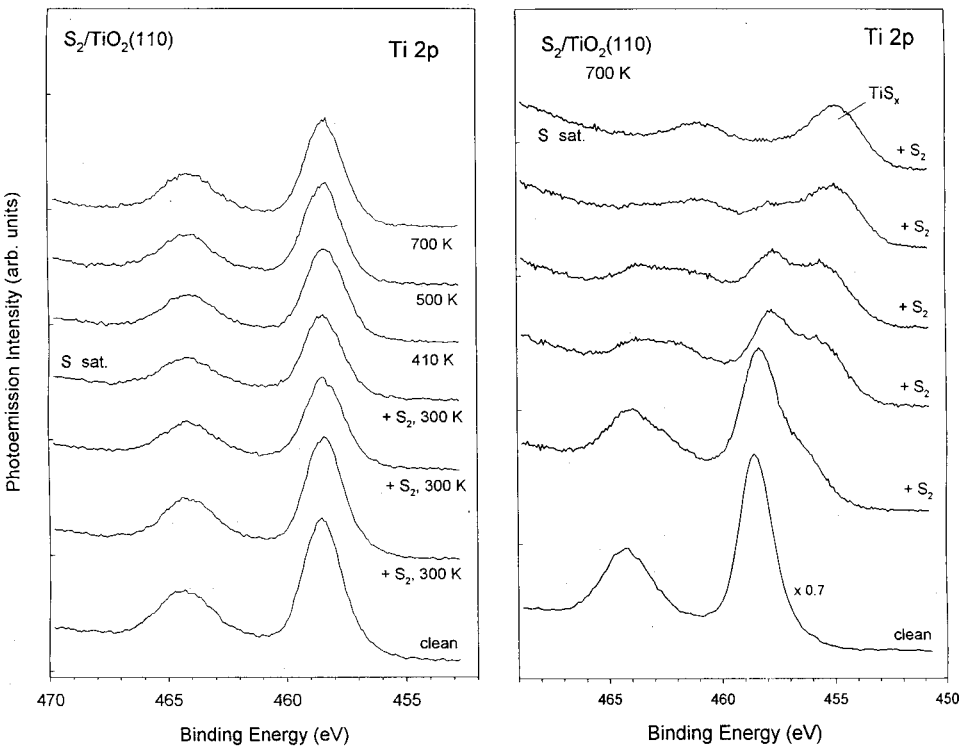

FIG. 5. Left side: Ti 2*p* photoemission spectra for the adsorption of sulfur on $TiO_2(110)$ at 300 K, with subsequent annealing to higher temperatures (300–700 K). Right side: Ti 2*p* spectra for the adsorption of sulfur on $TiO_2(110)$ at 700 K.

The results of thermal desorption indicate that the TiS_x aggregates are very stable on $TiO_2(110)$, decomposing at temperatures well above 1000 K. Figure 7 shows TDS results for the decomposition of the TiS_x formed after dosing sulfur to $TiO_2(110)$ at 800 K. The sample temperature was ramped to 1185 K (the highest temperature possible in our manipulator) and held there until the desorption rates of S, S_2, and SO began to decrease. Strong signals are observed for masses 32 (S) and 64 (S_2 or SO_2). From the initial rise of the mass 64 signal an apparent activation energy of 2.98 ± 0.03 eV is found for the decomposition process of the TiS_x. The negligible signal seen for the evolution of SO (a cracking fragment of SO_2) indicates that the mass 64 peak is essentially due to desorption of S_2. Although the oxide system is rich in sulfur, a reaction of the $S_{ads}+O_{surf}\rightarrow SO_{x,gas}$ type is not important, and should not contribute to the $O\leftrightarrow S$ exchange at the surface. Hebenstreit *et al.* have proposed that the exchange process could be facilitated by the migration of O vacancies or Ti^{3+} interstitials from the bulk to the surface of the oxide.[24,26] In the next section, we will examine these hypotheses by means of first-principles calculations.

B. Adsorption of sulfur on $TiO_2(110)$: Density functional studies

The $TiO_2(110)$ surface was represented by a four-layer slab as shown in Fig. 8, which was embedded in a three-dimensionally periodic supercell.[16,35] A vacuum of 12 Å was placed on top of the slab in order to ensure negligible interactions between periodic images normal to the surface.[16,33] Previous theoretical studies have shown that a three-layer

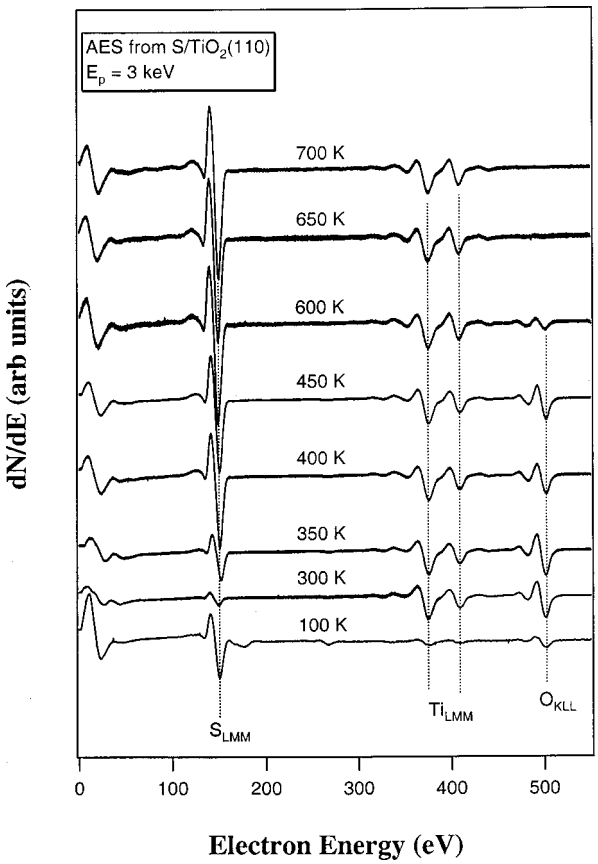

FIG. 6. Auger spectra acquired after saturating $TiO_2(110)$ with sulfur at different temperatures.

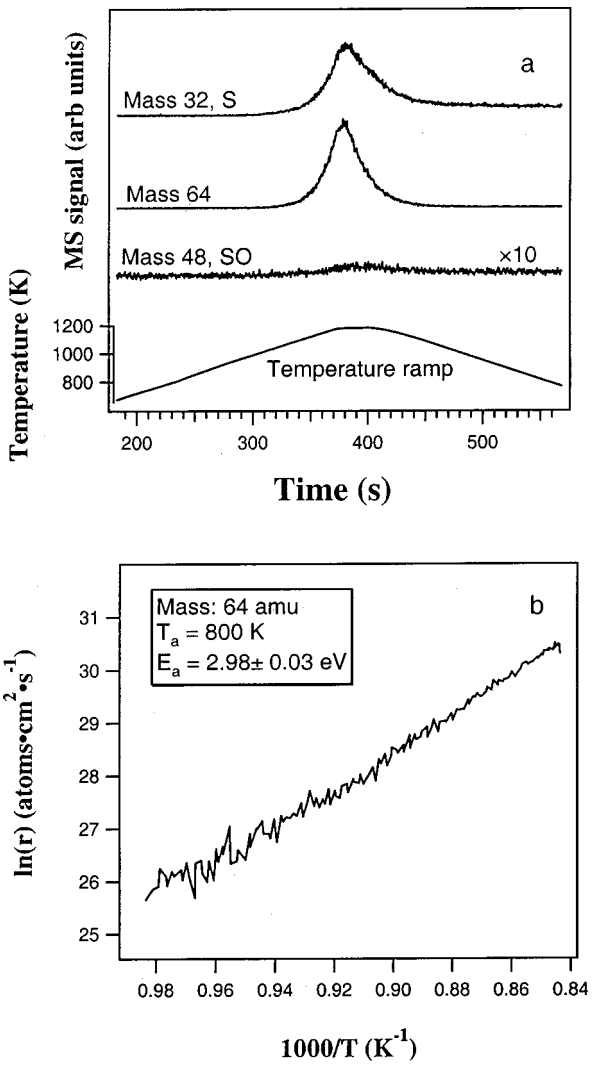

FIG. 7. Top: Thermal desorption spectra for the decomposition of a TiS_x overlayer formed after dosing sulfur to $TiO_2(110)$ at 800 K. Heating rate up to 1185 K: 2.7 K/s. Bottom: Activation energy for the decomposition of TiS_x.

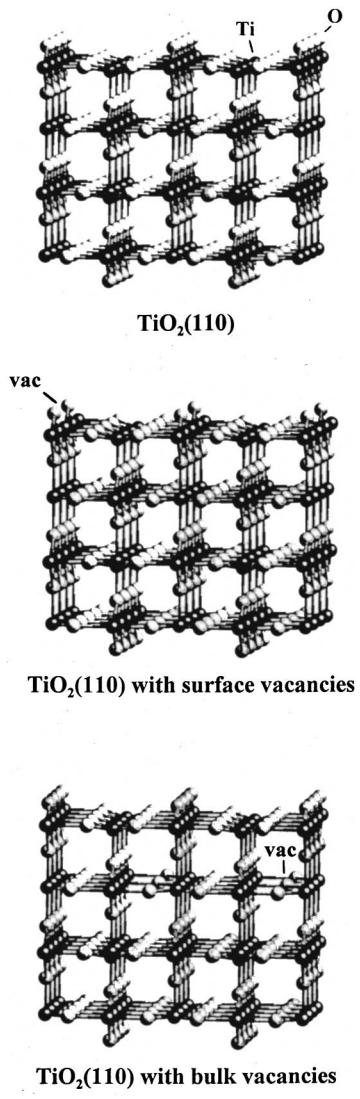

FIG. 8. Slabs used to model a perfect $TiO_2(110)$ surface (top), and systems with O vacancies in the surface (center) and subsurface (bottom) regions. Each slab contains four layers with Ti atoms. Ti atoms are represented by dark spheres, whereas gray spheres correspond to O atoms. The slab in the center corresponds to a (2×1)-$TiO_2(110)$ reconstructed surface.

periodic slab can reliably model adsorption reactions on a perfect $TiO_2(110)$ surface.[13,16,37–39,52] In our calculations, we added one more layer since we are also interested in examining the behavior of titania systems with vacancies on the surface and subsurface region.[33] The geometry optimization for bulk TiO_2 gave a rutile unit cell with $a=b=4.64$ Å and $c=2.97$ Å These values are close to those derived from experimental measurements[53] ($a=b=4.59$ Å, $c=2.96$ Å) and other theoretical calculations.[14,16,38] In the slab calculations the structural geometry of the first two layers was relaxed, while the other two layers were kept fixed in the geometry of bulk TiO_2. For the perfect $TiO_2(110)$ surface, the five- and sixfold-coordinated Ti ions moved in and out of plane by 0.15 and 0.11 Å, respectively. The bridging oxygens moved into the surface by 0.10 Å, and the in-plane oxygens moved out of the surface by 0.11 Å. These shifts in the atom positions agree well with those seen in other DF studies.[14,16,38] Most of them are also in good agreement with atomic shifts found in x-ray surface diffraction studies for $TiO_2(110)$,[54] the only exception being the shift for the bridging oxygens where the experimental results give a movement of 0.27 Å toward the surface.

To model a $TiO_2(110)$ surface with O vacancies, we used a four-layer periodic slab with atoms (50% or 25%) missing from the bridging oxygen rows in the first layer (see center of Fig. 8 for an example).[16,25,33] This is the most common position observed for O vacancies when their number is moderate or low.[1,24] In many situations it is unlikely that O vacancies in TiO_2 will assume a periodic array such as that shown in Fig. 8, but our model represents well the electronic perturbations associated with O vacancies (see below). The structural configuration seen in this model is usually known as a (2×1)-$TiO_2(110)$ reconstructed surface.[16] Here, the reduced surface is constructed by removing alternate bridging oxygens, giving a vacancy density of half a monolayer. The

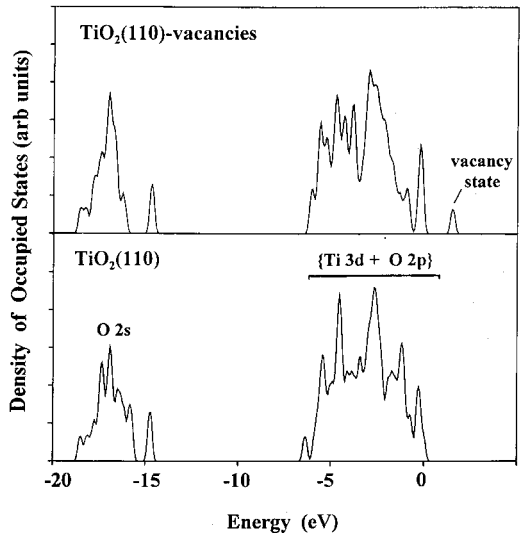

FIG. 9. Density functional results for the density of states of the occupied bands in $TiO_2(110)$ and a system with O vacancies in the surface, (2×1)-$TiO_2(110)$ reconstructed surface.

system could also adopt a (1×2) reconstruction that has the same density of vacancies, but now they form a complete missing row along the (001) direction.[16] Our DF calculations and previous theoretical work[16] show a small energy difference (<0.2 eV) between the (2×1) and (1×2) reconstructions. The (2×1)-$TiO_2(110)$ system is a better representation of a $TiO_2(110)$ surface with a moderate or low number of vacancies than the (1×2)-$TiO_2(110)$ system.[1,24] We also investigated the properties of a surface with a $p(2\times2)$ array of vacancies in the bridging oxygen rows. As in the case of the perfect $TiO_2(110)$ slab, the structural geometry of the first two layers in the slabs with surface O vacancies was relaxed while the bottom two layers were kept fixed in the geometry of bulk titania. In all cases, there was a substantial relaxation in the region near a missing oxygen with the adjacent Ti atoms moving downward and sideways (0.16–0.19 Å) to strengthen their bonds with the remaining oxygens.

Figure 9 displays the calculated density of states for the occupied bands in the perfect $TiO_2(110)$ slab and in the reduced (2×1)-$TiO_2(110)$ slab (surface with O vacancies in our notation, top panel). The valence band in $TiO_2(110)$ contains states of O $2p$ and Ti $3d$ character. Since the Ti-O bonds are not fully ionic and have a large degree of covalent character,[13–16] TiO_2 is best described as an ionocovalent oxide.[14] The introduction of O vacancies in the $TiO_2(110)$ surface generates a new occupied state that appears ~ 1.6 eV above the top of the $\{O2p+Ti3d\}$ band and has Ti $3d$ character. This state has been observed in experiments of valence photoemission,[1,26,55] and is frequently attributed to Ti^{3+} ions.[55] In the case of a (1×2)-$TiO_2(110)$ reconstructed surface, again we found an extra occupied state located ~ 1.2 eV above the TiO_2 valence band. Thus, from an electronic viewpoint, the Ti atoms located near O vacancies are better suited for electron-donor interactions with sulfur or other adsorbates than atoms in the Ti rows.

Table I lists structural parameters and bonding energies calculated for the adsorption of sulfur on perfect $TiO_2(110)$ and reduced oxide surfaces. On $TiO_2(110)$, the listed values are very similar to those found before using the same theoretical approach and a three-layer slab model.[25] Therefore, our main results are not an artifact of the thickness used for the slab model. Sulfur was adsorbed with coverages of 1.0, 0.5, and 0.25 ML, adopting $p(1\times1)$, $p(2\times1)$, or $p(2\times2)$ periodic overlayers. In our adsorption models, the geometry of the adsorbate and first two layers of the slab was allowed to relax during the DF calculations. The bonding energies for 0.5 and 0.25 ML of S increase according to the sequence bridging O rows<Ti rows<O vacancies, in agreement with the trends seen in the photoemission data of Figs. 1 and 2. It is known that the atoms in the bridging O rows of $TiO_2(110)$ bond SO_2 to form SO_3 and SO_4 species.[31] Indeed, the calculated bonding energy for S on these O centers is substantial (1.2–1.4 eV), but not large enough to compete with bonding to Ti sites. From the results in Table I, it is clear that S *must* bond preferentially to O vacancies of a $TiO_2(110)$ surface. Once these sites are saturated with S, then adsorption on the Ti rows should follow.

TABLE I. Adsorption of sulfur on $TiO_2(110)$: First-principles results.

	AC-S distance[a] (Å)	Adsorption energy[b] (eV)	Charge on S (e)
Perfect $TiO_2(110)$			
on Ti rows			
0.25 ML of S, $p(2\times2)$	2.41	2.91	−0.11
0.50 ML of S, $p(2\times1)$	2.46	2.60	−0.07
1.0 ML of S, $p(1\times1)$	2.61	1.34	−0.02
0.5 ML of S_2	2.69[c]	2.25	+0.11
on bridging O			
0.25 ML of S, $p(2\times2)$	1.60	1.38	+0.34
0.50 ML of S, $p(2\times1)$	1.63	1.21	+0.26
(2×1)-$TiO_2(110)$, vac			
on O vacancies			
0.25 ML of S, $p(2\times2)$	2.28	3.93	−0.33
0.50 ML of S, $p(2\times1)$	2.29	3.81	−0.28
(1×2)-$TiO_2(110)$, vac			
on O vacancies			
0.25 ML of S, $p(2\times2)$	2.24	3.97	−0.32
0.50 ML of S, $p(1\times2)$	2.26	3.89	−0.31
(2×2)-$TiO_2(110)$, vac			
on O vacancies			
0.25 ML of S, $p(2\times2)$	2.27	3.76	−0.26

[a]AC (adsorption center)=Ti in Ti rows or O vacancies, and O in bridging oxygen rows.

[b]The adsorption energies were calculated according to the expression $E_{ads}=E_S+E_{slab}-E_{(S+slab)}$, where E_S is the energy of an isolated S atom, E_{slab} is the total energy of the bare slab, and $E_{(S+slab)}$ is the total energy of the adsorbate/slab system. Positive adsorption energies denote an exothermic adsorption process.

[c]The S-S bond length was 1.95 Å on the oxide surface versus 1.90 Å in the free S_2 molecule.

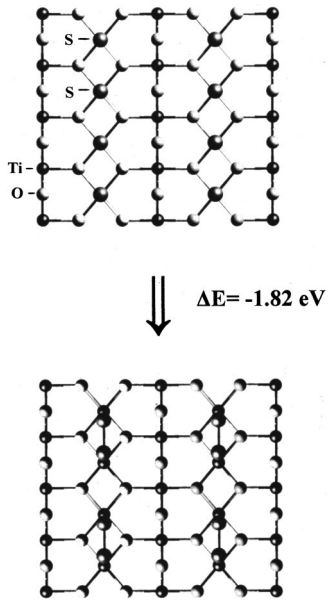

FIG. 10. View from the top for a full monolayer of sulfur on a perfect $TiO_2(110)$ surface. Dark spheres denote Ti atoms. The O and S atoms are represented by small and large gray spheres, respectively. Initially, the S atoms were directly above the metal atoms in the Ti rows (therefore these Ti atoms are not visible in this top view). Upon full relaxation of the system, adjacent sulfur atoms moved to form S_2 molecules.

On the Ti rows, there is a large drop in the adsorption energy with increasing S coverage, and for large coverages the calculations predict that chemisorbed S_2 molecules are more stable than S atoms. Figure 10 illustrates this in detail for the case of a $TiO_2(110)$ surface saturated with sulfur. Initially, a monolayer of atomic S is on the Ti rows, and upon complete relaxation the S atoms pair forming dimers ($\Delta E = -1.82$ eV, exothermic process). At this coverage the Ti-S bonds are not strong enough and the system gains stability by forming S-S bonds. In the adsorbed S_2 molecules, the S-S bond length (1.94 Å) is somewhat larger than that found for free S_2 (1.90 Å). To desorb these S_2 species as molecules one has to put only 0.59 eV into the system. Thus, in photoemission experiments, evidence for the presence of S_2 species on $TiO_2(110)$ was found only upon dosing of the adsorbate at temperatures well below 300 K. For the adsorption of sulfur on the O vacancy sites of a (2×1)-$TiO_2(110)$ surface, we found that S_2 pairs were not stable with respect to atomic S. This was also true for sulfur on O vacancy sites of a (1×2)-$TiO_2(110)$ surface, even when the missing rows of bridging oxygens were completely replaced by rows of bridging sulfur atoms. In these cases, there was a drop in the adsorption energy of S with increasing coverage, but the Ti-S bonds at the O vacancies were still strong enough to prevent S-S bonding.

In Table I an interesting trend is observed in the projected Mulliken charges[47] for adsorbed sulfur. The electron density on the sulfur atoms increases in the order S on bridging O$<$$S_2$ on Ti rows$<$S on Ti rows$<$S on O vacancies. The fact that Ti atoms near O vacancies are better electron donors than atoms in the normal Ti rows of the surface can be expected from the differences seen in the density-of-states plots of Fig. 9. Following the standard model for core-level shifts based on changes in electron-electron repulsion,[56] one can expect that the smaller the electron density on a sulfur atom, the higher the binding energy of its $2p$ core levels. And indeed, comparing the results in Fig. 2 and Table I, one finds a nice qualitative correlation between the charge and binding energy of the $2p$ levels of adsorbed sulfur. However, this must be taken with caution since several factors can affect the position of the core levels of an atom on a surface.[56–58] In general, the bond between S and the oxide surface is best described as covalent, with a small degree of ionic character. As the S coverage increases, the degree of ionicity in the S-TiO_2 bond decreases.

The migration of O vacancies from the bulk to the surface of $TiO_2(110)$ could be the key pathway for the formation of a TiS_x overlayer.[24,26] After cleaning/preparing a titania sample, one obtains a distribution of O vacancies from the surface to the bulk of the system.[1,24,59] Using the two-slab models shown at the center and bottom of Fig. 8, we compared the stability of O vacancies in the surface and subsurface regions of $TiO_2(110)$. After structural relaxation of the top two layers in each slab, the DF calculations predict a small difference in stability (0.13 eV) that favors the structure with subsurface vacancies. If one compares with a (1×2)-$TiO_2(110)$ system instead of a (2×1)-$TiO_2(110)$ system, then the difference in stability between surface and subsurface vacancies is almost zero. In all cases, the calculated energy differences are small and well within the accuracy of the method. When S adatoms (0.5 ML) are present on the surface, the migration of O vacancies from the subsurface region to the surface (see Fig. 11) is a highly exothermic process ($\Delta E = -0.89$ or -1.11 eV), which certainly can lead to formation of TiS_x aggregates on $TiO_2(110)$. DF calculations for 0.25 ML of S on $TiO_2(110)$ slabs that initially contained subsurface O vacancies in $p(2\times1)$ and $p(2\times2)$ arrays also showed a substantial release of energy ($>$0.5 eV) upon diffusion of the vacancies to the surface. Although this process is well downhill from a thermodynamic viewpoint, it probably needs elevated temperatures to overcome activation energies associated with the migration path of the O vacancies.[4]

A second route for the formation of TiS_x on $TiO_2(110)$ could involve the migration of Ti^{3+} interstitials.[26] These species originate as a result of an excess of Ti in the titania lattice,[59,60] and in some situations they are known to exhibit a faster mobility than O vacancies.[60] The exact position of the Ti^{3+} interstitials in the TiO_2 lattice is unknown. Using DF and relaxed slab models, we calculated the ΔE for the migration path shown in Fig. 12 and proposed in Ref. 26. In this system, initially, 0.5 ML of interstitial titanium are below the surface, with 0.5 ML of S atoms on the surface. Without the sulfur, a subsurface$\rightarrow$surface migration of the titanium interstitials is highly endothermic ($\Delta E = +1.06$ eV) due to the overall rupture of Ti-O bonds. The formation of a Ti-S bond is not enough to compensate for the breaking of Ti-O bonds, and the Ti migration in Fig. 12 is still an uphill process ($\Delta E = +0.27$ eV). This trend did not change when a larger cell was used in the DF calcula-

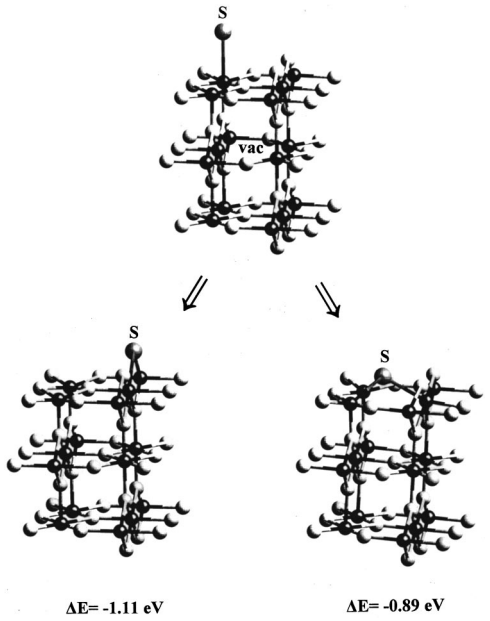

FIG. 11. Sulfur-induced migration of O vacancies. Initially, S is adsorbed on the Ti rows and O vacancies are located in the subsurface or bulk region. In the final state, the O vacancies have moved to the surface (bridging O rows, left, or in-plane positions, right) and are ''covered'' by S atoms. In the scheme, only three of the four layers in the slab models are shown. Ti atoms are represented by dark spheres, whereas gray spheres correspond to O atoms.

tions and 0.25 ML of S adatoms coexisted with 0.25 ML of Ti interstitials ($\Delta E = +0.38$ eV). Our DF calculations indicate that an exothermic subsurface→surface migration of Ti can be obtained at large concentrations of Ti interstitials ($\theta_S = 0.5$ ML and $\theta_{Ti(int)} \geqslant 0.75$ ML; initially substantial strain within the TiO_2 lattice occurs due to the large amount of Ti interstitials) or big coverages of S adatoms ($\theta_{Ti(int)} = 0.5$ ML and $\theta_S \geqslant 0.75$ ML; multiple Ti-S bonds upon Ti migration). Such conditions are not easy to achieve in the experiments of Fig. 5. Therefore, the migration of O vacancies (Fig. 11) clearly appears as a much better route for the generation of TiS_x on $TiO_2(110)$. This is consistent with the experimental trends seen in photoemission and AES spectroscopy for the disappearance of the O signal near the surface during the sulfidation reaction. In the migration processes of Fig. 11, there is no substantial loss of Ti-O bonding and strong Ti-S bonds are gained.

IV. DISCUSSION

The first-principles calculations in Sec. III B indicate that the bond between S and pentacoordinated Ti atoms of TiO_2 is mainly covalent. Charges derived from a particular partition scheme of the electron density should not be considered in absolute quantitative terms,[47,57,61] but from the results in Table I it is quite clear that the charge separation in the S-TiO_2 bond is small. In bulk TiO_2, the Ti-O bonds are not fully ionic and have a large degree of covalent character.[13–16] For a S atom on an O vacancy the calculated Mulliken charge ($\sim -0.3e$) was substantially smaller than that observed for O atoms in the same position ($\sim -0.55e$). This can be expected due to the large difference in the Pauling electronegativities of S [2.58 (Ref. 62)] and O [3.44 (Ref. 62)]. As compounds, sulfides are known to be less ionic than oxides.[63] The trend in the relative ionicity of the Ti-O and Ti-S bonds is consistent with the shift seen in Fig. 5 for the Ti $2p$ core levels after O↔S exchange at high temperature.

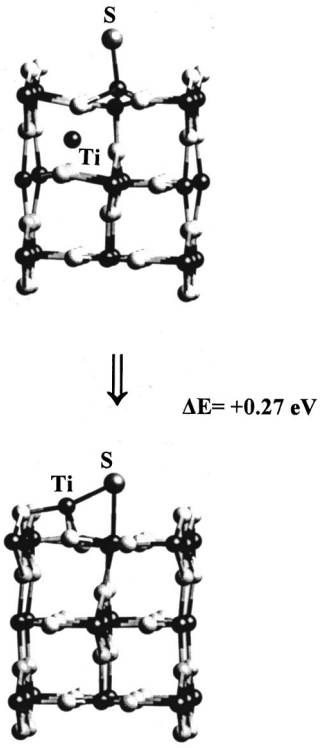

FIG. 12. Migration of Ti^{3+} interstitials in the presence of sulfur. Initially, S (0.5 ML) is adsorbed on the Ti rows and excess Ti atoms (0.5 ML) are located in the subsurface or bulk region. In the final state, the excess Ti atoms have moved to the surface and are bonded to S atoms. In the scheme, only three of the four layers in the slab models are shown. All Ti atoms are represented by dark spheres, whereas gray spheres correspond to O atoms.

The sulfur↔oxide bonding interactions observed on $TiO_2(110)$ are much stronger than those previously found for the adsorption of sulfur on highly ionic oxides like MgO(100) (Ref. 23) and Al_2O_3.[64] They are similar to those found on ZnO(0001),[23] another ionocovalent compound like TiO_2.[14,63] In principle, several phenomena can affect the bonding of an adsorbate on an oxide surface: band-orbital hybridizations and subsequent electron transfer between adsorbate and surface, effects of Pauli repulsion, charge polarization induced by adsorption, attractive electrostatic interactions between the charge on the adsorbate and the Madelung field of the oxide, etc.[1,9–13] The behavior seen for sulfur on the oxide surfaces reflects the importance of band-orbital interactions for the adsorption and bonding of this element. Oxides that have a large degree of ionicity usually have a wide band gap, with bands that are either too stable (valence states) or unstable (conduction states) for effective bonding interactions with most adsorbates.[9,23] According to a simple model based on band-orbital mixing,[9,42,65] the smaller the

band gap in an oxide, the bigger its activity for adsorption processes. Thus, TiO_2 with a small band gap[1] (BG$\sim$3 eV) is more reactive than MgO [BG$\sim$7 eV (Ref. 23)] or Al_2O_3 [BG$\sim$9 eV (Ref. 64)]. The same model also explains the differences in reactivity observed between perfect and vacancy-rich $TiO_2(110)$. The creation of O vacancies in $TiO_2(110)$ produces states above the valence $\{O2p+Ti3d\}$ band, effectively reducing the band gap of the oxide (see Fig. 9) and making it more reactive.

Recent theoretical studies have demonstrated the important role that oxygen vacancies play in the behavior of highly ionic oxides like MgO or Al_2O_3.[3–8] For example, the metal and O centers of a perfect MgO(100) surface exhibit extremely weak interactions with many adsorbates.[1,3,11,42] The reactivity of the surface drastically changes in the presence of O vacancies.[3,5,8,11] O vacancies induce electronic states within the band gap of the oxide,[3–5] and at high concentrations lead to the appearance of metallicity in the surface layer.[4] In $MgO_{1-x}(100)$, the excess electronic charge is highly localized on the O vacancy sites[3,4,12] and a large fraction of it can be transferred to adsorbates.[3,5,8] Thus, the SO_2 molecule picks up more than a full electron upon adsorption and breaks apart on the oxide surface.[5] Also, Pd atoms bonded to $MgO_{1-x}(100)$ acquire a big negative charge ($\sim -0.9e$) and exhibit quite unusual chemical properties.[3,8] In a much less ionic oxide like TiO_2, the degree of charge localization on the O vacancy sites is less pronounced and part of the excess electronic charge is distributed on the neighboring cations.[14–16,66] This charge delocalization seems to affect the bonding of adsorbates. Sulfur atoms bonded to O vacancy sites of $TiO_{2-x}(110)$ do no receive a large charge from the oxide substrate. Interestingly, the results of photoemission and density functional calculations show that adsorbed sulfur atoms completely suppress the Ti^{3+} states seen in the valence spectra of $TiO_{2-x}(110)$ surfaces.[25,26] The removal of these electronic states is mainly a consequence of covalent interactions between the S $3p$ and Ti $3d$ orbitals and not the result of a large oxide$\rightarrow$S charge transfer.

The interactions between S and the O vacancies of TiO_2 are complex. On one hand, the O vacancies greatly enhance the adsorption energy of S on the oxide surface. On the other hand, the adsorbed S substantially affects the relative stability of O vacancies in the surface and subsurface regions of the oxide substrate. The second phenomenon can lead to unexpected chemical transformations. From a thermodynamic viewpoint, sulfides are less stable than oxides.[67] A bulk transformation of the type $S_2(gas)+TiO_2(bulk)\rightarrow TiS(bulk)+SO_2(gas)$ is highly endothermic[67] ($\Delta H=+280.5$ kJ/mol or 2.9 eV). Our TDS results show that such reactions will not occur on a $TiO_2(110)$ surface either. However, the migration of O vacancies from the bulk to the surface of the oxide makes possible a $TiO_2\rightarrow TiS_x$ transformation. The experimental and theoretical results in Sec. III together with the STM data in Ref. 26 indicate that a vacancy-mediated sulfidation process can play an important role in the poisoning (catalysis) or passivation (electronic-device protection) of oxide surfaces by sulfur. Furthermore, not only sulfur adatoms can induce the migration of subsurface oxygen vacancies in TiO_2. Recent studies in our laboratory show that NO_2 and N_2O also induce this phenomenon.[33,68] The same is valid for Cl adatoms.[26] Even an admetal like Au, which bonds weakly to stoichiometric $TiO_2(110)$,[69,70] favors a subsurface$\rightarrow$surface migration of O vacancies.[68] Supporting evidence for a vacancy-mediated reduction process is also found in the reaction of H_2 with NiO(100).[71] Subsurface defects can induce the ''rosette restructuring'' of the $TiO_2(110)$ substrate[59,72] and affect the adsorption and dissociation of O_2.[73,74] Thus, when dealing with adsorption processes on an oxide, one must take into consideration the subsurface composition and the possible exchange of defects between the bulk and surface of the system.

The results in Fig. 6 indicate that the temperature is an important parameter in the generation of TiS_x on titania. In oxides[1,4] and other solids,[75,76] the diffusion of bulk vacancies is associated with an activation energy: the higher the temperature, the faster the rate of exchange of O vacancies between the bulk and surface of the oxide. The growth of the sulfide layer is limited by the diffusion of O vacancies to the surface, since a bulky sulfur atom cannot penetrate and diffuse into the bulk of rutile. In this respect, the thermodynamically unlikely surface sulfidation is self-limiting. Different self-limiting film growth modes are known for reactions between gases and solids[77] but they do not involve the phenomena seen here for the $TiS_x/TiO_2(110)$ system.

V. CONCLUSIONS

The S $2p$ core levels are very sensitive to the adsorption site of sulfur on $TiO_2(110)$. Upon adsorption of S_2 at temperatures between 100 and 300 K, high-resolution photoemission shows several types of sulfur species on the surface: SO_x groups, S atoms bonded to the Ti rows or on O vacancies in the bridging oxygen rows, and S_n aggregates. The amount of SO_x formed is very small and the S_n aggregates are seen only upon adsorption below room temperature.

The S atoms bond much more strongly to O vacancy sites than to atoms in the Ti rows of a perfect oxide surface. The electronic states associated with Ti^{3+} sites favor bonding to S, but there is not a substantial oxide$\rightarrow$adsorbate charge transfer. In general, the bond between S and the Ti cations is best described as covalent, with a small degree of ionic character. As the sulfur coverage increases, the degree of ionicity in the S-TiO_2 bond decreases further. During TDS the S atoms bonded to the Ti rows desorb as molecular S_2 between 350 and 500 K. In contrast, only evolution of atomic S is observed for the desorption of S bonded on O vacancies ($T>600$ K).

For dosing of S at high temperatures ($>$500 K) a layer of TiS_x is formed on $TiO_2(110)$. The O signal disappears in photoemission and Auger spectroscopy, and the Ti $2p$ core levels show a complete $TiO_2\rightarrow TiS_x$ transformation in the surface and subsurface regions. The O$\leftrightarrow$S exchange does not involve the production of SO or SO_2 species. The formation

of TiS_x involves the migration of O vacancies from the bulk to the surface. The $S/TiO_2(110)$ system illustrates how important surface *and* subsurface defects can be in the behavior of an oxide surface. The generation of TiS_x on titania is a clear example of how surface segregation of O vacancies in an oxide can drive chemical transformations that would be impossible in a stoichiometric material.

ACKNOWLEDGMENTS

This research was carried out at Brookhaven National Laboratory under Contract No. DE-AC02-98CH10086 with the U.S. Department of Energy (Division of Chemical Sciences). The NSLS is supported by the Divisions of Materials and Chemical Sciences of DOE.

*Corresponding author. FAX: 1-631-344-5815. Email address: rodrigez@bnl.gov

[1] V. E. Henrich and P. A. Cox, *The Surface Science of Metal Oxides* (Cambridge University Press, Cambridge, 1994).
[2] C. Noguera, *Physics and Chemistry at Oxide Surfaces* (Cambridge University Press, Cambridge, 1995).
[3] L. Giordano, J. Goniakowski, and G. Pacchioni, Phys. Rev. B **64**, 075417 (2001).
[4] F. Finocchi, J. Goniakowski, and C. Noguera, Phys. Rev. B **59**, 5178 (1999).
[5] J. A. Rodriguez, T. Jirsak, L. Gonzalez, J. Evans, M. Perez, and A. Maiti, J. Chem. Phys. **115**, 10 914 (2001).
[6] A. Bogicevic and D. R. Jennison, Phys. Rev. Lett. **82**, 4050 (1999); Surf. Sci. **437**, L741 (1999).
[7] W. F. Schneider, J. Li, and K. C. Hass, J. Phys. Chem. B **105**, 6972 (2001).
[8] S. Abbet, A. Sanchez, U. Heiz, W.-D. Schneider, A. M. Ferrari, G. Pacchioni, and N. Rösch, J. Am. Chem. Soc. **122**, 3453 (2000).
[9] J. A. Rodriguez, Theor. Chem. Acc. **107**, 117 (2002).
[10] H. J. Freund, Faraday Discuss. **114**, 1 (1999).
[11] G. Pacchioni, Surf. Rev. Lett. **7**, 277 (2000).
[12] G. Pacchioni, A. M. Ferrari, and G. Ierano, Faraday Discuss. **106**, 155 (1997).
[13] G. Pacchioni, A. M. Ferrari, and P. S. Bagus, Surf. Sci. **350**, 159 (1996).
[14] T. Albaret, F. Finocchi, and C. Noguera, Faraday Discuss. **114**, 285 (1999).
[15] S. Bartkowski, M. Neumann, E. Z. Kurmaev, V. V. Fedorenko, S. N. Shamin, V. M. Cherkashenko, S. N. Nemmonov, A. Winiarski, and D. C. Rubie, Phys. Rev. B **56**, 10 656 (1997).
[16] P. J. D. Lindan, N. M. Harrison, M. J. Gillan, and J. A. White, Phys. Rev. B **55**, 15 919 (1997).
[17] A. Sherman, *Chemical Vapor Deposition for Microelectronics: Principles, Technology and Applications* (Noyes Publications, Park Ridge, NJ, 1987).
[18] J. A. Rodriguez and J. Hrbek, Acc. Chem. Res. **32**, 719 (1999).
[19] C. N. Satterfield, *Heterogeneous Catalysis in Practice* (McGraw-Hill, New York, 1980).
[20] A. V. Slack and G. A. Holliden, *Sulfur Dioxide Removal from Waste Gases*, 2nd ed. (Noyes Data Corporation, Park Ridge, NJ, 1975).
[21] A. Piéplu, O. Saur, J.-C. Lavalley, O. Legendre, and C. Nédez, Catal. Rev. - Sci. Eng. **40**, 409 (1998).
[22] C. Muryn, D. Purdie, P. Hardman, A. L. Johnson, N. S. Prakash, G. N. Raiker, G. Thorton, and D. Law, Faraday Discuss. Chem. Soc. **89**, 77 (1990).
[23] J. A. Rodriguez and A. Maiti, J. Phys. Chem. B **104**, 3630 (2000).
[24] E. L. D. Hebenstreit, W. Hebenstreit, and U. Diebold, Surf. Sci. **461**, 87 (2000); **470**, 347 (2001).
[25] J. A. Rodriguez, J. Hrbek, J. Dvorak, T. Jirsak, and A. Maiti, Chem. Phys. Lett. **336**, 377 (2001).
[26] E. L. D. Hebenstreit, W. Hebenstreit, H. Geisler, C. A. Ventrice, P. T. Sprunger, and U. Diebold, Surf. Sci. **486**, L467 (2001).
[27] J. Hrbek, J. A. Rodriguez, J. Dvorak, and T. Jirsak, Collect. Czech. Chem. Commun. **66**, 1149 (2001).
[28] K. E. Smith, J. L. Mackay, and V. E. Henrich, Phys. Rev. B **35**, 5822 (1987).
[29] K. E. Smith and V. E. Henrich, J. Vac. Sci. Technol. A **7**, 1967 (1989).
[30] D. I. Sayago, P. Serrano, O. Bohme, A. Goldoni, G. Paolucci, E. Roman, and J. A. Martin-Gago, Phys. Rev. B **64**, 205402 (2001).
[31] D. R. Warburton, D. Pundie, C. A. Muryn, K. Prahakaran, P. L. Wincott, and G. Thorton, Surf. Sci. **269/270**, 305 (1992), and references therein.
[32] J. A. Rodriguez, S. Chaturvedi, T. Jirsak, and J. Hrbek, J. Chem. Phys. **109**, 4052 (1998), and references therein.
[33] J. A. Rodriguez, T. Jirsak, G. Liu, J. Hrbek, J. Dvorak, and A. Maiti, J. Am. Chem. Soc. **123**, 9597 (2001).
[34] V. Milman, B. Winkler, J. A. White, C. J. Pickard, M. C. Payne, M. C. , E. V. Akhmatskaya, and R. H. Nobes, Int. J. Quantum Chem. **77**, 895 (2000).
[35] M. C. Payne, D. C. Allan, T. A. Arias, and J. D. Johannopoulus, Rev. Mod. Phys. **64**, 1045 (1992).
[36] I. Dawson, P. D. Bristowe, M. H. Lee, M. C. Payne, M. D. Segall, and J. White, Phys. Rev. B **54**, 13 727 (1996).
[37] P. J. D. Lindan, N. M. Harrison, J. M. Holender, and M. J. Gillan, Chem. Phys. Lett. **261**, 246 (1996).
[38] D. C. Sorescu and J. T. Yates, J. Phys. Chem. B **102**, 4556 (1998).
[39] D. C. Sorescu, C. N. Rusu, and J. T. Yates, J. Phys. Chem. B **104**, 4408 (2000).
[40] K. Refson, R. A. Wogelius, D. G. Fraser, M. C. Payne, M. H. Lee, and V. Milman, Phys. Rev. B **52**, 10 823 (1995).
[41] J. A. Rodriguez, J. C. Hanson, S. Chaturvedi, A. Maiti, and J. L. Brito, J. Chem. Phys. **112**, 935 (2000).
[42] J. A. Rodriguez, T. Jirsak, M. Pérez, L. González, and A. Maiti, J. Chem. Phys. **114**, 4186 (2001).
[43] D. Vanderbilt, Phys. Rev. B **41**, 7892 (1990).
[44] H. J. Monkhorst and J. D. Pack, Phys. Rev. B **13**, 5188 (1976).
[45] J. A. White and D. M. Bird, Phys. Rev. B **50**, 4954 (1994).
[46] J. P. Perdew, K. Burke, and Y. Wang, Phys. Rev. B **54**, 16 533 (1996).
[47] M. D. Segall, C. J. Pickard, R. Shah, and M. C. Payne, Phys. Rev. B **54**, 16 317 (1996).
[48] J. A. Rodriguez, T. Jirsak, S. Chaturvedi, and M. Kuhn, Surf. Sci. **442**, 400 (1999), and references therein.
[49] J. A. Rodriguez, S. Chaturvedi, and M. Kuhn, Surf. Sci. **415**, L1065 (1998).
[50] J. A. Rodriguez, J. Hrbek, M. Kuhn, T. Jirsak, S. Chaturvedi, and A. Maiti, J. Chem. Phys. **113**, 11 284 (2000).
[51] H. Gutleben and E. Bechtold, Surf. Sci. **191**, 157 (1987).

[52] Z. Yang, R. Wu, Q. Zhang, and D. W. Goodman, Phys. Rev. B **63**, 045419 (2001).
[53] S. C. Abrahams and J. L. Bernstein, J. Chem. Phys. **55**, 3206 (1971).
[54] G. Charlton, P. B. Howes, C. L. Nicklin, P. Steadman, J. S. G. Taylor, C. A. Muryn, S. P. Harte, J. Mercer, R. MacGrath, D. Norman, T. S. Turner, and G. Thorton, Phys. Rev. Lett. **78**, 495 (1997), and references therein.
[55] H. R. Sadeghi and V. E. Henrich, J. Catal. **109**, 1 (1988), and references therein.
[56] W. F. Egelhoff, Surf. Sci. Rep. **6**, 253 (1987).
[57] M. Weinert and R. E. Watson, Phys. Rev. B **51**, 17 168 (1995).
[58] Z. Yang, R. Wu, and J. A. Rodriguez, Phys. Rev. B **65**, 155409 (2002).
[59] M. Li, W. Hebenstreit, U. Diebold, A. M. Tyrishkin, M. K. Bowman, G. G. Dunham, and M. A. Henderson, J. Phys. Chem. B **104**, 4944 (2000).
[60] M. A. Henderson, Surf. Sci. **419**, 174 (1999).
[61] K. B. Wiberg and P. R. Rablen, J. Comput. Chem. **14**, 1504 (1993).
[62] J. Emsley, *The Elements* (Oxford University Press, Oxford, 1989).
[63] J. C. Phillips, *Bonds and Bands in Semiconductors* (Academic, New York, 1973).
[64] J. A. Rodriguez, S. Chaturvedi, M. Kuhn, and J. Hrbek, J. Phys. Chem. B **102**, 5511 (1998).
[65] R. Hoffmann, *Solids and Surfaces: A Chemist's View of Bonding in Extended Structures* (VCH, New York, 1988).
[66] M. Ramamoorthy, R. D. King-Smith, and D. Vanderbilt, Phys. Rev. B **49**, 7709 (1994).
[67] *Lange's Handbook of Chemistry*, 13th ed., edited by J. A. Dean (McGraw-Hill, New York, 1985), Sec. 9.
[68] J. A. Rodriguez, G. Liu, T. Jirsak, J. Hrbek, Z. Chang, J. Dvorak, and A. Maiti, J. Am. Chem. Soc. **124**, 5242 (2002).
[69] M. Valden, X. Lai, and D. W. Goodman, Science **281**, 1647 (1998).
[70] L. Zhang, F. Cosandey, R. Persaud, and T. E. Madey, Surf. Sci. **439**, 73 (1999).
[71] J. A. Rodriguez, J. C. Hanson, A. Frenkel, J. Y. Kim, and M. Perez, J. Am. Chem. Soc. **124**, 346 (2002).
[72] U. Diebold, M. Li, O. Dulub, E. L. D. Hebenstreit, and W. Hebenstreit, Surf. Rev. Lett. **7**, 613 (2000).
[73] M. Li, W. Hebenstreit, U. Diebold, M. A. Henderson, and D. R. Jennison, Faraday Discuss. **114**, 245 (1999).
[74] M. Li, W. Hebenstreit, L. Gross, U. Diebold, M. A. Henderson, D. R. Jennison, P. A. Schultz, and M. P. Sears, Surf. Sci. **437**, 173 (1999).
[75] K. F. McCarty, J. A. Nobel, and N. C. Bartelt, Nature (London) **412**, 622 (2001).
[76] B. Meyer and M. Fahnle, Phys. Rev. B **59**, 6072 (1999).
[77] S. R. Qiu, H. F. Lai, and J. A. Yarmoff, Phys. Rev. Lett. **85**, 1492 (2000), and references therein.